Journal of
MATERIALS RESEARCH

Welcome Comments Help

Laser-processing-induced phase transformation in Zn–Al-based alloy

Y.H. Zhu
Instituto de Investigaciones en Materiales, Universidad Nacional Autonoma de Mexico, Mexico D.F., Mexico, and Department of Manufacturing Engineering, Hong Kong Polytechnic University, Hong Kong, People's Republic of China

J.A. Chavez-Carvayar
Instituto de Investigaciones en Materiales, Universidad Nacional Autonoma de Mexico, Mexico D.F., Mexico

H.C. Man
Department of Manufacturing Engineering, Hong Kong Polytechnic University, Hong Kong, People's Republic of China

M. Villagran
Centro de Instrumentos, Universidad Nacional Autonoma de Mexico, Mexico D.F., Mexico

(Received 4 November 1998; accepted 19 July 1999)

Microstructure and phase transformation of a furnace-cooled eutectoid Zn–Al-based alloy were studied after laser beam bombardment using low-angle x-ray diffraction (XRD) and backscattered scanning electron microscopy (BSEM). It was found that the microstructure of the laser-beam-treated specimen consisted mainly of the supersaturated Zn-rich β'_s phase particulates of about 1–2 μm in diameter. Three structure morphologies were observed. Microcracking occurred in the laser-beam-affected zone during laser processing. Two laser-processing-induced phase transformations, i.e., decomposition of the η'_{FC} phase and a four-phase transformation, were detected using XRD and BSEM techniques, similar to phase transformations that occurred in the same eutectoid Zn–Al-based alloy after various thermal and thermomechanical processing procedures.

I. INTRODUCTION

Laser processing is one of the advanced technologies in materials science and engineering. One of the most important applications of laser processing is surface alloying of the materials in order to improve their mechanical and physical properties, such as tensile strength, creep resistance, fatigue strength and hardness, etc.[1,2] The main processes involved in this new technology are rapid heating and rapid solidification of the alloy surface, by which a better microstructure such as fine grain structure and some intermediate phases could form and enhance the mechanical and physical properties of the alloy surface.

Al-based alloys have important advantages as structural materials because of their low density and high strength. The big obstacle for the application of the Al-based alloys is the low hardness of the alloys. Attempts at applying the Al-based alloys for pistons are attractive in case the surface hardness can be enhanced using laser cladding and alloying with some intermediate compounds or phases of fairly high hardness. It was reported that a rhombohedral T′ phase (Zn10A135Cu55 in wt%) enhanced hardness of the Zn–Al–Cu alloys.[3–6] It is a possible alternative compound for cladding on the Al alloys. Also it was reported that the T′ phase formed via a four-phase transformation: $\alpha + \epsilon \rightarrow T' + \eta$ in the prolonged aging of the Zn–Al–Cu alloys. Therefore the laser-processing-induced microstructural change and phase transformation of the Zn–Al–Cu alloys become interesting topics. Unfortunately little work has been found in laser processing of Zn–Al–Cu alloys.

In the present work the microstructure of a furnace-cooled eutectoid Zn–Al-based alloy was investigated after laser processing. Also the related phase transformation that occurred during laser processing was studied.

II. EXPERIMENTAL

An eutectoid Zn–Al-based alloy ingot of 12 mm in diameter was solution treated at 350 °C for 4 days, then furnace cooled (FC) to ambient temperature inside the furnace chamber. The nominal composition of the alloy was Zn76A122Cu2 (in wt%).

The solution-treated and furnace-cooled specimens were polished prior to laser processing. The laser processing was carried out on the polished FC alloy speci-

 © 1999 Materials Research Society

CAMBRIDGE JOURNALS
http://journals.cambridge.org Downloaded: 27 Aug 2013 IP address: 158.132.161.52

mens using a neodymium–yttrium aluminum garnet (Nd–YAG) Laser Surelite with an energy of 170 mJ. The laser radiation had a wavelength of $\lambda = 1.06$ μm (near to infrared) and 6 mm in beam diameter. In order to study the laser-processing-induced microstructural change, various numbers of laser beam treatment were selected as 10, 30, 50, and 70 pulses. The pulse repetition rate was 1 Hz with a pulse width of 5 ns. The as-laser-beam-treated specimens were then examined immediately after each laser processing.

Backscattered scanning electron microscopy (BSEM) was applied for examination of the microstructures of both the FC and the laser-beam-treated specimens to obtain a distinct atomic contrast between various phases involved. The ground and polished FC specimens were for BSEM examination. The as-FC specimens were scanned on a Philips x-ray diffractometer with nickel-filtered Cu K_α radiation, $\lambda = 1.5406$ A and a scanning speed was 1 ° 2θ per min. A low-angle x-ray diffraction (XRD) technique was applied to detect the crystal structure of the laser-beam-treated surface of the alloy specimens. The as-laser-treated specimens were scanned on a Siemens D5000 x-ray diffractometer with Cu K_α radiation and a scanning speed of 0.1° 2θ per min. A range of diffraction was selected from 35° to 47° 2θ for both the XRD and the low-angle XRD.

For comparison, the FC eutectoid Zn–Al-based alloy specimens were examined after various periods of aging at 150 °C. Also various parts of a 150 °C tensile specimen were examined using XRD and BSEM. The detailed procedures for both the aging and the tensile deformation at 150 °C were reported in previous papers.[7]

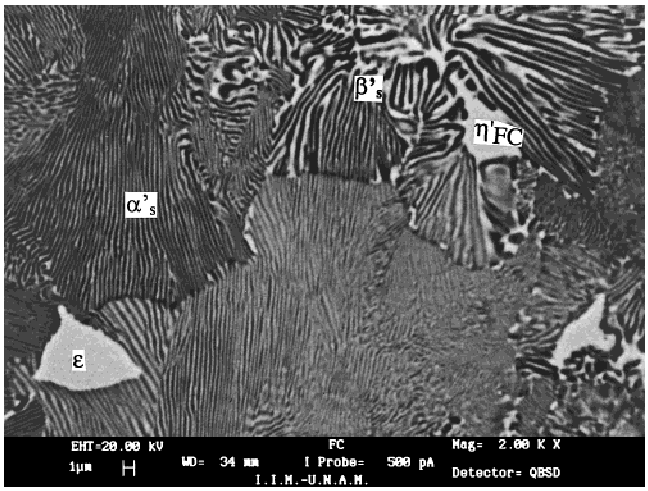

(a)

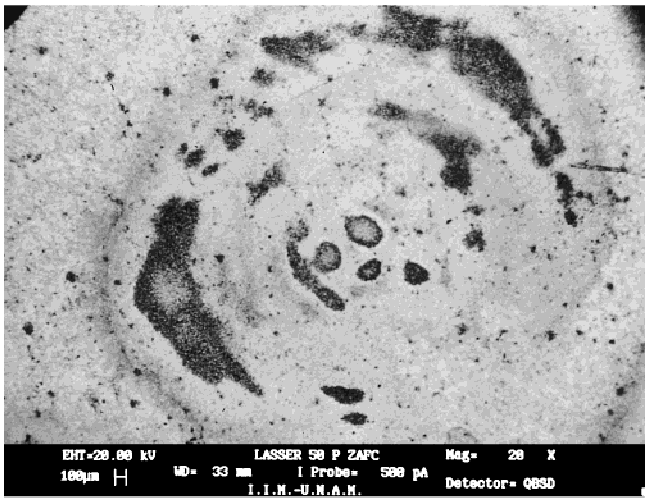

(b)

FIG. 1. (a) Backscattered electron image of the FC eutectoid Zn–Al-based alloy. (b) Backscattered electron image of the laser-beam-treated specimen.

III. RESULTS AND DISCUSSION

A. Microstructure of as-FC eutectoid Zn–Al-based alloy

There were two phases of β and ϵ in the solution-treated eutectoid Zn–Al-based alloy at 350 °C.[8] These two phases became unstable and decomposed to various Al-rich and Zn-rich metastable phases during furnace cooling. Because the decomposition rates of Al-rich and the Zn-rich phases were quite different, coarse lamellae and fine lamellae formed, as labeled by α'_s and β'_s in Fig. 1(a) respectively. The resultant microstructure consisted of coarse lamellae and fine lamellae, and the Zn-rich η'_{FC} and ϵ (Zn_4Cu) phase particles. The microstructure of the as-FC specimen is shown in Fig. 1(a), where both Zn-rich η'_{FC} and ϵ phases were lightly contrasted in the backscattered scanning electron microscopy (SEM) image. It was found that the η'_{FC} phase decomposed slightly during furnace cooling, and dark-imaged α phase precipitates formed at the η'_{FC} phase boundaries.

Three metastable phases, face-centered-cubic [(fcc) Al-rich phase] α, η'_{FC}, and ϵ, existed in the furnace-cooled eutectoid Zn–Al-based alloy, as shown in the x-ray diffractogram Fig. 2(a), where the characteristic diffraction peaks of the phases are separately indexed.

The phases involved in this study are listed in Table I.

B. Microstructural change after laser treatment

Microstructure of as-laser-beam-treated specimens mainly consisted of the supersaturated Zn-rich β'_s phase particulates of about 1–2 μm in diameter, in addition to an eutectic structure of dark-imaged α particles and light-imaged η'_{FC} phase in the interparticulate region, as shown in Fig. 3. A similar fine particulate structure was obtained in a cast ingot from a wedge-shaped mould with a cooling rate range about 1000–1500 K/s.[10] Because of rapid cooling the melt directly solidified at the β phase field in the phase diagram and formed Zn-rich supersatu-

CAMBRIDGE JOURNALS
http://journals.cambridge.org Downloaded: 27 Aug 2013 IP address: 158.132.161.52

rated β'_s. The supersaturated β'_s phase particulate structure is a structural characteristic of the rapid-cooled eutectoid Zn–Al-based alloy.

Because of the uneven intensity distribution of the laser bombarded, different structure morphologies were observed in the laser-beam-bombed (50 pulses) specimen, as shown in Fig. 1(b). Shown in Fig. 4 are three different microstructures in the specimens after 50-pulse laser-beam treatment, i.e., the fine particulate structure, a columnar structure, and an intermediate grown particulate structure. The strongly affected zone appeared as a columnar structure, but the fine particulate structure was the principal microstructure.

This supersaturated β'_s phase decomposed quickly during rapid heating from the subsequent laser treatments. Repeatedly the laser-beam treatments resulted in further decomposing and growing of the β'_s phase particulates into the columnar structure. Various backscattered SEM images of the specimens after 10, 30, 50, and 70 pulses of laser-beam treatments are shown in Fig. 5. It

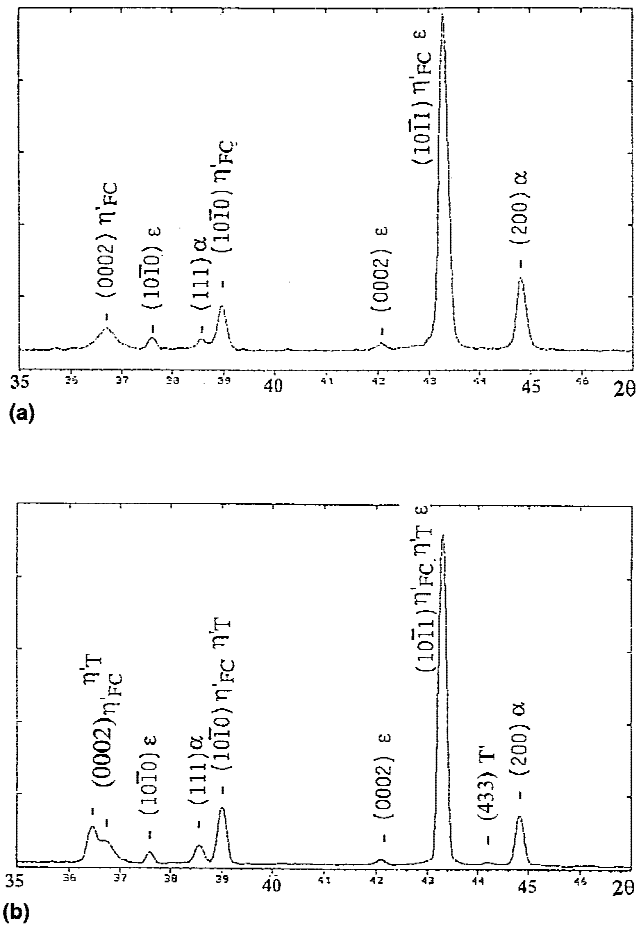

FIG. 2. (a) X-ray diffractogram of the FC eutectoid Zn–Al-based alloy. (b) X-ray diffractogram of the laser-beam-affected surface layer of 2-μm thickness, using low-angle XRD.

TABLE I. List of phases.

Equilibrium	
α	Al-rich fcc phase
β	Zn-rich fcc phase
ϵ	Hexagonal-close-packed (hcp) phase $CuZn_4$
η	Zn-rich hcp phase
T′	Rhombohedral phase Zn10A135Cu55 (in wt%)
Nonequilibrium	
β'_s	Supersaturated Zn-rich fcc phase
α'_s	Supersaturated Al-rich fcc phase
α	Relative stable Al-rich fcc phase
ϵ	hcp phase $CuZn_4$
η'_{FC}	Supersaturated Zn-rich hcp phase in FC Zn–Al alloy
η'_T	Metastable Zn-rich hcp phase
η	Relative stable Zn-rich hcp phase
T′	Rhombohedral phase Zn10A135Cu55 (in wt%)

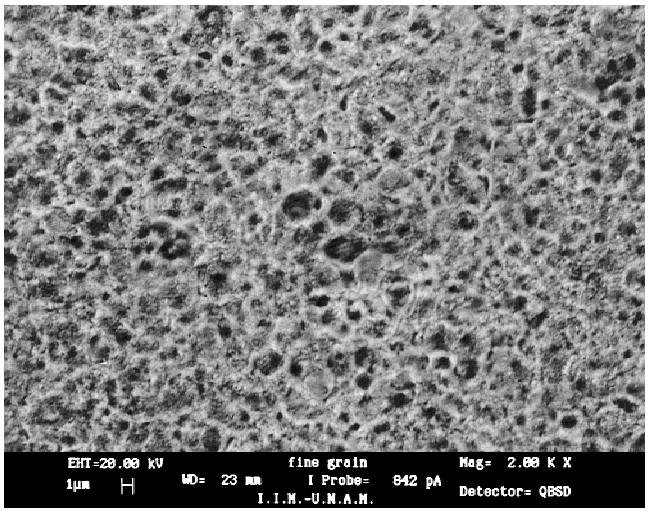

FIG. 3. Backscattered electron image of the as-laser-beam-treated alloy specimen, showing the main microstructure of the supersaturated β'_s phase particulates of about 1–2 μm in diameter.

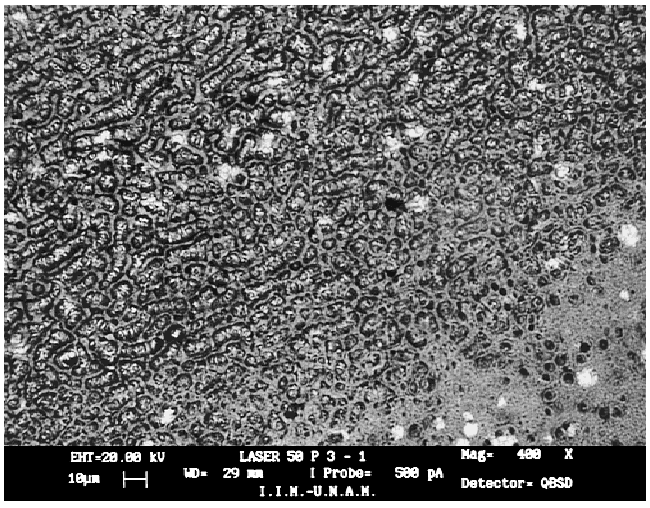

FIG. 4. Backscattered electron image of the as-laser-beam-treated alloy specimen, showing three different microstructures after 50 pulses of laser-beam treatment.

CAMBRIDGE JOURNALS
http://journals.cambridge.org Downloaded: 27 Aug 2013 IP address: 158.132.161.52

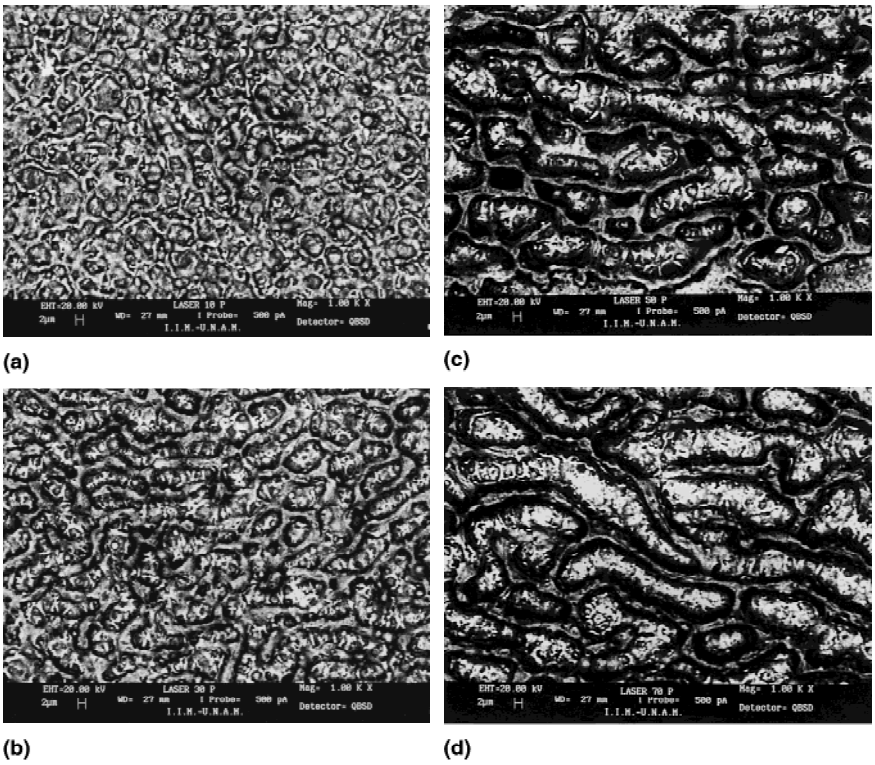

FIG. 5. Various backscattered electron images of the as-laser-beam-treated alloy specimen after 10, 30, 50, and 70 pulses of laser-beam treatment.

was clearly observed that the columns of the decomposed β'_s phase had grown with increasing number of laser-beam treatments. The columns of the decomposed β'_s phase were about 10 μm in diameter after 70 pulses of laser-beam treatment. A similar columnar structure of the decomposed β'_s phase was observed in the edge of the continuous cast ingot of the eutectoid Zn–Al-based alloy, where the cooling rate of the ingot was very high at the wall of a water-jet cooled mold. The composition of the β'_s phase columnar was Zn72Al25Cu3 (in wt%).[11]

The laser-beam-affected zone was found to be about 25–30 μm in thickness depending on the intensity of the laser beam and the number of the laser-beam treatment, as shown in the BSEM images of the cross section of the laser-treated specimen, Figs. 6(a) and 6(b). Microcracking occurred in the laser-beam-affected zone (50-pulse bombing) at the surface of the specimen, as shown in Figs. 6(a) and 6(b). A major reason for cracking is that during laser processing the surface of the specimen was heated rapidly and the laser-beam-produced energy might be sufficiently high for evaporation of the Zn-rich η'_{FC} phase of low melting point locally, forming microvoids at the surface. The cracking may started from the imperfection of the surface because of a restrained contraction of the melt pool during rapid solidification afterwards. A high cooling rate always generates high residual thermal stresses that further enhance the danger of hot crack formation.[12,13]

C. Phase transformation

The laser-beam-treated specimen was examined using low-angle XRD technique. It was found that the surface layer of 2-μm thickness consisted of η'_T, α, and ε phases, as shown in Fig. 2(b). Compared with the diffractogram of the as-FC specimen bulk, shown in Fig. 2(a), it was clear that the η'_{FC} phase decomposed at the laser-treated surface of the specimen. At the lower 2θ angle a (0002) diffraction peak of metastable η'_T occurred, while the original (0002) diffraction peak of the η'_{FC} decreased in intensity, as shown in Fig. 2(b).

Another phase transformation was also detected. The (433) diffraction peak of the T′ phase appeared at 2θ 44.3° of the x-ray diffractogram of the laser-beam-treated specimen, accompanying intensity decreasing of both $(10\bar{1}0)$ and (0002) diffraction of the ε phase, as shown in Fig. 2(b). This is a well-recognized phenomenon of a four-phase transformation, $\alpha + \epsilon \rightarrow T' + \eta$.

These two phase transformations, the decomposition of the η'_{FC} phase and the four-phase transformation, have been detected repeatedly in the specimens during various thermal and thermomechanical treatments.[7,9,14–19] In comparison, the x-ray diffractograms of the same eutectoid Zn–Al-based alloy specimens at various stages of aging at 100 °C and of various parts of the specimen after tensile deformation at 150 °C are shown in Figs. 7 and 8 respectively.[7,9]

CAMBRIDGE JOURNALS
http://journals.cambridge.org Downloaded: 27 Aug 2013 IP address: 158.132.161.52

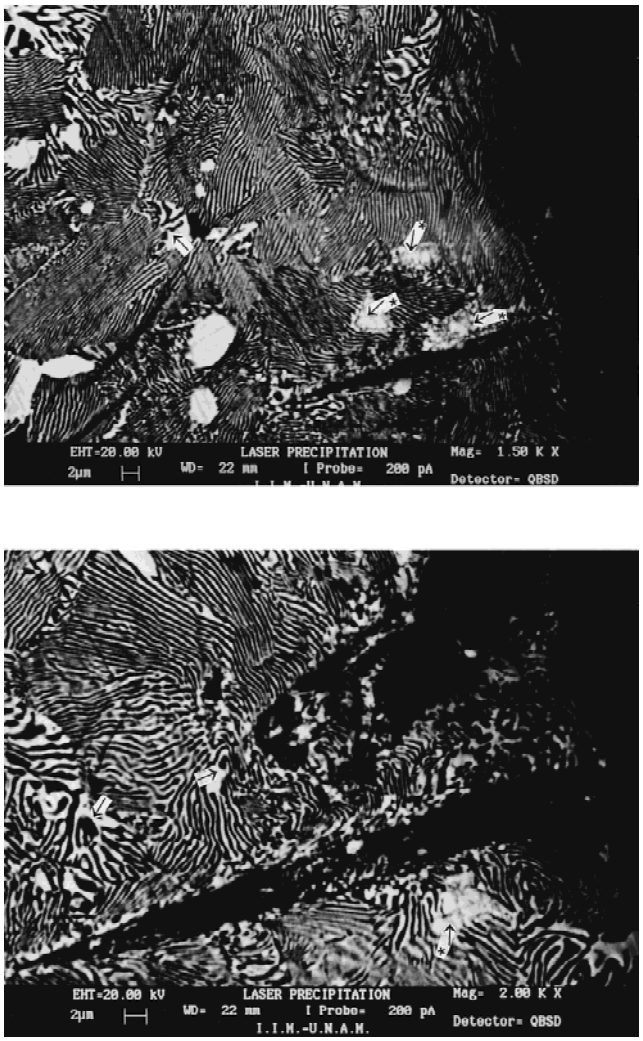

FIG. 6. Backscattered electron images of the cross section of the as-laser-beam-treated alloy specimen, showing microcracking in the laser-beam-affected zone (50 pulses). Arrows and arrows with asterisks represent the precipitates of the α and T′ phases respectively.

Figure 8 shows clearly that the (0002) diffraction peak of the η'_{FC} phase decreased in height, while the (0002) diffraction peak of a metastable η'_{T} phase appeared and increased during aging. Meanwhile both diffraction intensities of the α and ϵ phases decreased in height. The decomposition of the η'_{FC} phase occurred at an early stage of aging, as a discontinuous precipitation, $\eta'_{FC} \rightarrow \eta'_{T} + \alpha + \epsilon$. The four-phase transformation, $\alpha + \epsilon \rightarrow T' + \eta$, occurred during the prolonged aging.

Under the external tensile deformation, similar phase transformations were observed. As shown in Fig. 8, the discontinuous decomposition of the η'_{FC} phase was clearly detected in the neck zone and the rupture part of the specimen, where the specimen suffered a high strain. In the rupture part of the specimen, the (433) diffraction peak of the T′ phase was clearly formed, whereas the diffraction peaks of the ϵ phase decreased in height. This meant that a higher external stress induced the four-phase transformation in the tensile-deformed eutectoid Zn–Al based alloy.

The above-mentioned two-phase transformations were observed using BSEM. The dark-imaged α phase precipitates were observed in the laser-beam-affected zone; arrows represent them in BSEM images of the cross section of the specimen in Figs. 6(a) and 6(b). This was a characteristic of the decomposition of the η'_{FC} phase. The decomposition of the η'_{FC} phase occurred as a discontinuous precipitation, $\eta'_{FC} \rightarrow \eta'_{T} + \alpha + \epsilon$, in the early stage of aging, which was followed by a continuous precipitation.[7]

The four-phase transformation, $\alpha + \epsilon \rightarrow T' + \eta$, was characteristic of the formation of the gray-imaged T′ phase precipitates inside the light-imaged ϵ phase. As marked by arrows with asterisks in Figs. 6(a) and 6(b), the T′ phase precipitates were observed in the laser-

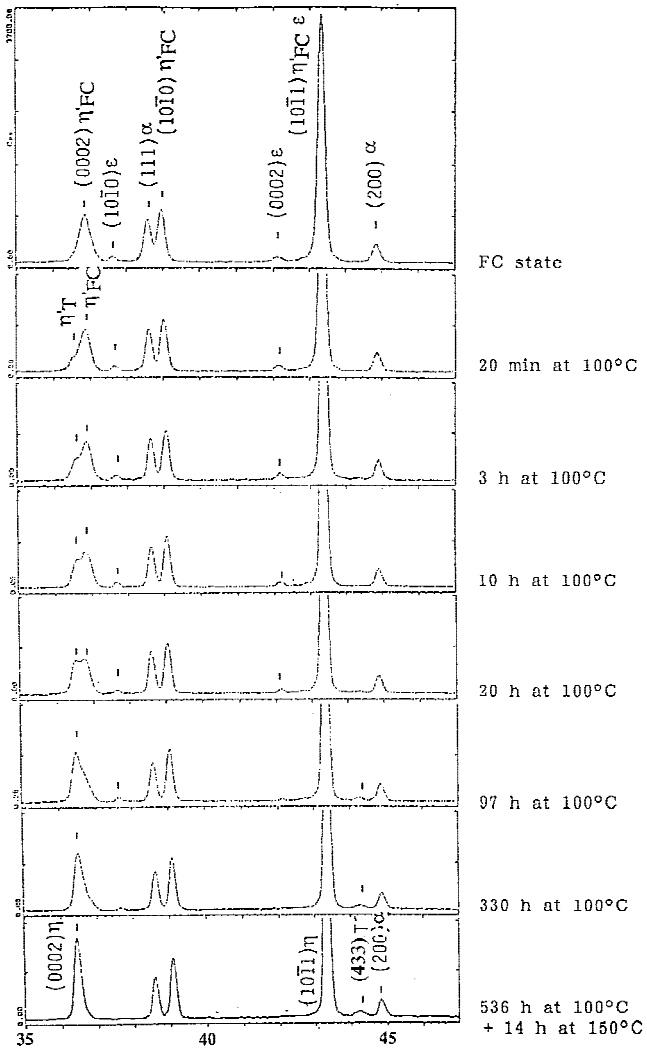

FIG. 7. X-ray diffractograms of the FC eutectoid Zn–Al-based alloy after various stages of aging at 150 °C.

CAMBRIDGE JOURNALS
http://journals.cambridge.org Downloaded: 27 Aug 2013 IP address: 158.132.161.52

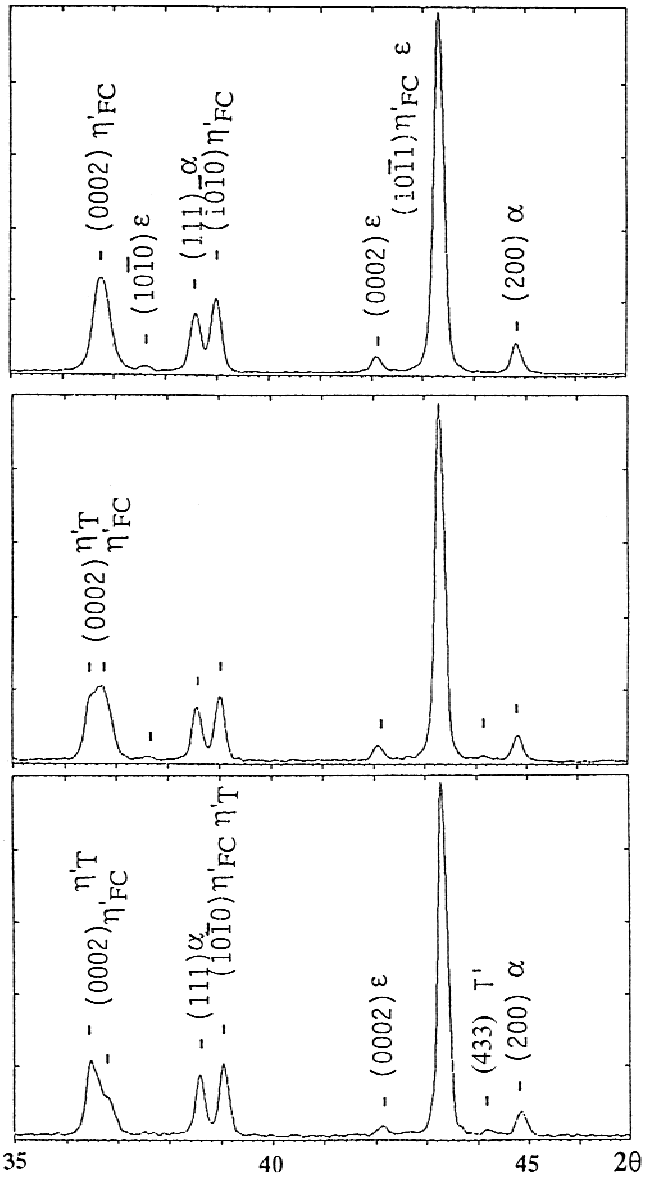

FIG. 8. X-ray diffractograms of various parts of the FC eutectoid Zn–Al-based alloy after tensile testing at 150 °C.

beam-affected zone at the surface of the specimen. Because the α phase contained more light Al and less heavy Cu than the T′ phase, a distinct atomic contrast between the α phase and the T′ phase was received on the BSEM images. The former appeared as dark-imaged precipitate and the latter was gray in color. It was also found that there was no precipitation of the T′ phase outside the laser-beam-affected zone of the specimen about 30 μm from the surface, as shown in Fig. 6(a).

For comparison, the BSEM image of the FC eutectoid Zn–Al-based alloy specimen after 30-h aging at 150 °C is shown in Fig. 9. Both the similar dark-imaged α phase precipitates and the gray-imaged T′ phase precipitates are marked by the arrow and arrows with asterisks, respectively. These two typical morphologies for the above-mentioned phase transformations were also reported in previous investigations.[7,20,21]

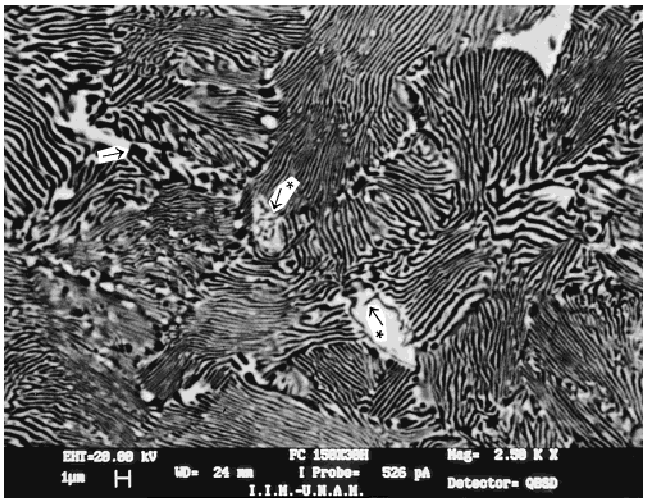

FIG. 9. Backscattered electron image of the FC eutectoid Zn–Al-based alloy after 30 h ageing at 150 °C. Arrow and arrows with asterisks represent the precipitates of the α and T′ phases respectively.

During laser processing the T′ phase formed in the Zn–Al-based alloy. According to previous investigation,[3–6] the T′ phase enhanced the hardness of the Zn–Al-based alloy. Thus the formation of the T′ phase using laser processing could be one of the alternative practical methods for the surface hardening of the Zn–Al-based and the Al-based alloys.

IV. CONCLUSIONS

(1) Because of rapid solidification and cooling, the fine particulate structure of the supersaturated β'_s phase appeared as the main structure in the laser-beam-treated FC eutectoid Zn–Al-based alloy.

(2) Due to an uneven intensity distribution of the laser beam, three structure morphologies were observed: the fine particulate structure, the columnar structure, and the intermediate grown particulate structure.

(3) Microcracking occurred in the laser-beam-affected zone at the surface of the alloy specimen.

(4) The decomposition of the η'_{FC} phase, $\eta'_{FC} \rightarrow \eta'_T + \alpha + \epsilon$, and the four-phase transformation, $\alpha + \epsilon \rightarrow T' + \eta$, were detected in the laser-beam-affected surface of the FC eutectoid Zn–Al-based alloy.

ACKNOWLEDGMENTS

The authors thank DGAPA de Universidad Nacional Autonoma de Mexico for financial support (Project No. IN503797) and also Dr. C. Garcia, Dr. P. Quintana, L. Baños, Antonio Caballero, and Jose Guzman for their assistance in experimental work.

CAMBRIDGE JOURNALS
http://journals.cambridge.org Downloaded: 27 Aug 2013 IP address: 158.132.161.52

REFERENCES

1. W.M. Steen, in *Laser Material Processing* (Springer Verlag, New York, 1991), Chaps. 1, 2, and 4.
2. J. Powell, H. Engstron, and C. Magnusson, Fabricator **May,** 80 (1994).
3. R. Ciach, J. Krol, and K. Wegrzyn-Tasior, Bull. Acad. Polon. Sci. (Tech.) **17,** 371 (1969).
4. J. Krol and K. Wegrzyn-Tasior, Arch. Hutn. **16,** 119 (1971).
5. S. Murphy, Z. Metallkd. **71,** 96 (1980).
6. Y.H. Zhu, Chin. J. Mater. Sci. Technol. **6,** 125 (1990).
7. Y.H. Zhu, H.C. Man, H.J. Dorates, and R.M. Hernandez, in *Proceedings of the Fourth International Conference Advances in Materials and Processing Technologies, Kuala Lumpur, Malaysia, 24–28 August 1998* edited by A.M. Hamouda, S. Sulaiman, and M. Ahmadun (Sirim Press, Kuala Lumpur, 1998), Vol. 1, pp. 89–96.
8. Y.H. Zhu, H.C. Man, and W.B. Lee, Mater. Sci. Eng. A **268,** 147 (1999).
9. Y.H. Zhu, J. Torres, and W.B. Lee (unpublished).
10. Y.H. Zhu, J. Torres, J.L. Reyes, J.A. Juarez-Islas, and L. Banos, J. Mater. Sci. Eng. A **226–228,** 33 (1997).
11. Y.H. Zhu (unpublished).
12. A.A. Junai, M. van Dijk, M. Hienich, A. Rijnders, G. Notenboom, and G. Jelmorini, Proc. SPIE **1277,** 217 (1990).
13. W. Golderer, R. Schwab, and R. Stutzle, Welding and Cutting **12,** E211 (1985).
14. Y.H. Zhu and F.E. Goodwin, J. Mater. Res. **10,** 1927 (1995).
15. Y.H. Zhu and E. Orozco, Metall. Mater. Trans. A **26,** 2611 (1995).
16. Y.H. Zhu and J. Torres, Z. Metallkd. **88,** 329 (1997).
17. Y.H. Zhu, E. Orozco, and J. Torres, Mater. Trans., JIM **38,** 521 (1997).
18. Y.H. Zhu and J. Torres, J. Mater. Proc. Technol. **73,** 25 (1998).
19. Y.H. Zhu, V.M. Lopez Hirata, and M. Sauced Munoz, Z. Metallkd. **88,** 934 (1997).
20. Y.H. Zhu, Metals and Materials **4,** 878 (1998).
21. Y.H. Zhu, R.M. Hernandez, and L. Banoz, J. Mater. Sci. **34,** 1 (1999).

CAMBRIDGE JOURNALS
http://journals.cambridge.org Downloaded: 27 Aug 2013 IP address: 158.132.161.52